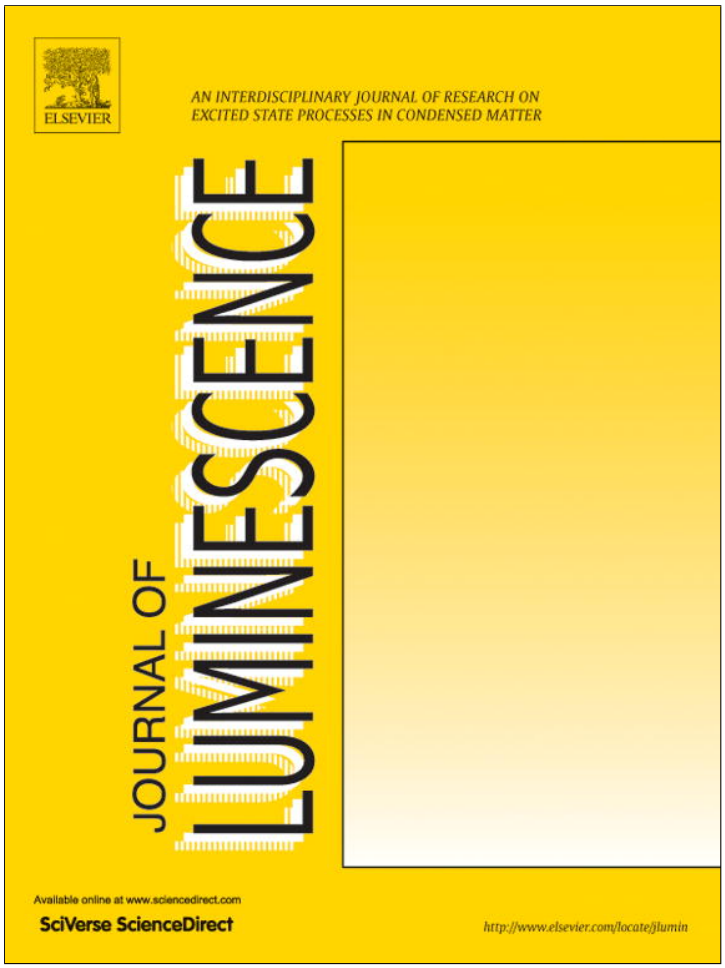

(This is a sample cover image for this issue. The actual cover is not yet available at this time.)

Journal of Luminescence 132 (2012) 2730–2735

Contents lists available at SciVerse ScienceDirect

Journal of Luminescence

journal homepage: www.elsevier.com/locate/jlumin

Interactions between imazethapyr and bovine serum albumin: Spectrofluorimetric study

Maria E. Pacheco, Liliana Bruzzone *

División Química Analítica, Departamento de Química, Facultad de Ciencias Exactas, Universidad Nacional de La Plata, La Plata, Buenos Aires, Argentina

ARTICLE INFO

Article history:
Received 29 December 2011
Received in revised form
2 May 2012
Accepted 18 May 2012
Available online 26 May 2012

Keywords:
Bovine serum albumin
Imazethapyr
Fluorescence quenching
Thermodynamic parameters

ABSTRACT

The interaction between imazethapyr (IMA) and bovine serum albumin (BSA) was investigated by fluorescence spectroscopy. The Stern–Volmer quenching constant (K_{SV}) at three temperatures was evaluated in order to determine the quenching mechanism. The dependence of fluorescence quenching on viscosity was also evaluated for this purpose. The results showed that IMA quenches the fluorescence intensity of BSA through a static quenching process. The values of the binding constant for the formed BSA–IMA complex and the number of binding sites were found to be $1.51 \times 10^5\ M^{-1}$ and 0.77, respectively, at room temperature. Based on the calculated thermodynamic parameters, the forces that dominate the binding process are hydrogen bonds and van der Waals forces, and the binding process is spontaneous and exothermic. The quenching of protein fluorescence by iodide ion was used to probe the accessibility of tryptophan residues in BSA and the change in accessibility induced by the presence of IMA. According to the obtained results, the BSA–IMA complex is formed in the site where the Trp-134 is located, causing it to become less exposed to the solvent.

1. Introduction

Imazethapyr—IMA—(5-ethyl-2-[(RS)-4-isopropyl-4-methyl-5-oxo-2-imidazolin-2-yl] nicotinic acid; Fig. 1) is an imidazolinone class herbicide that inhibits acetolactate synthase, which regulates plant growth. It is a pre-emergence and post-emergence herbicide, and it can be applied before the plant is incorporated. It is used to control major annual and perennial grass and broad-leaved weeds in soya beans and other leguminous crops.

Serum albumin is the most abundant plasma protein in human and other mammals. It is essential for maintaining the osmotic pressure needed for proper distribution of body fluids between intravascular compartments and body tissues [1].

Bovine and human serum albumins display approximately 76% sequence homology. The bovine serum albumin (BSA) molecule is made up of three homologous domains (I, II and III) which are divided into nine loops by 17 disulphide bonds. Each domain in turn is the product of two subdomains. The albumin structure is predominantly α-helical. BSA has two tryptophan (Trp) residues: Trp-134 in the first domain and Trp-212 in the second domain [2]. Trp-212 is located within a hydrophobic binding pocket of the protein and Trp-134 is located on the surface of the molecule. Human serum albumin (HSA) is a globular protein composed of three structurally similar domains (I, II and III), each containing two subdomains and stabilized by 17 disulphide bridges. From the spectroscopic point of view the main difference between the two proteins is that human serum albumin has only one tryptophan residue (Trp-214), while bovine serum albumin contains two: Trp-212 and Trp-134 [3]. Tryptophan and tyrosine residues present in the protein act as intrinsic fluorescence probes.

Several chemical substances bind reversibly to albumin and other serum components, which then function as carriers. In this work, we selected BSA because of its abundance, low cost and ligand-binding properties.

Spectrometric techniques, such as UV–visible absorption and fluorescence, can provide valuable information when interactions between small molecules and proteins are studied. Steady state fluorescence techniques were employed to make a detailed and insightful study on the interactions between BSA and IMA. The involved mechanism of fluorescence quenching was determined using the Stern–Volmer equation and according to the obtained results a further investigation of the main process responsible for the decrease in BSA emission was performed. The accessibility of tryptophan residues in the presence and absence of a ligand (IMA) was studied by KI quenching.

2. Experimental

2.1. Reagents and chemicals

Bovine serum albumin, BSA (Cohn Analog, ≥98%: Sigma-Aldrich), was dissolved in 0.10 M Tris–HCl buffer solution (pH=7.4),

* Corresponding author. Tel.: +54 221 4228328; fax: +54 221 4254533.
E-mail address: bruzzone@quimica.unlp.edu.ar (L. Bruzzone).

0022-2313/$ - see front matter © 2012 Elsevier B.V. All rights reserved.
http://dx.doi.org/10.1016/j.jlumin.2012.05.023

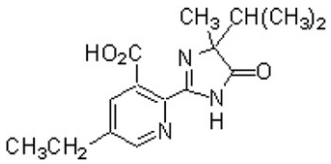

Fig. 1. Molecular structure of IMA.

containing 0.15 M NaCl, to prepare a stock solution (1.28×10^{-4} M) which was then stored at 0–4 °C for a maximum period of three months.

Imazethapyr (IMA) was provided by a local industry. The IMA stock solution, 1.00×10^{-3} M, was prepared daily by dissolving the herbicide in buffer solution (pH=7.4).

All chemicals were analytical-grade reagent and all solutions were prepared using double-distilled water.

2.2. Apparatus

All recordings of fluorescence spectra and fluorescence measurements were carried out on a Perkin–Elmer LS-50B luminescence spectrometer (Beaconsfield, England) equipped with a pulsed xenon lamp (half peak height <10 μs, 60 Hz), an R928 photomultiplier tube and a computer working with FL Winlab software. All measurements were performed in a 1.0 cm pathlength quartz cell and the excitation and emission bandwidths were set at 5 nm.

Absorption spectra were measured on a Shimadzu UV-240 (Japan) recording spectrophotometer, equipped with a 1.0 cm pathlength quartz cell.

The solutions were maintained at the desired temperature using a Lauda (Germany) K2R cryostat.

3. Results and discussions

3.1. Absorption spectra

The absorbance spectrum of IMA shows a broad and slightly structured band with two maxima at around 208 nm and 275 nm (Fig. 2). It overlaps with the absorbance spectrum of BSA (Fig. 2), which presents two broad bands at 227 nm and 280 nm.

3.2. Fluorescence study

For proteins, tyrosine (Tyr) and tryptophan (Trp) residues provide intrinsic fluorescence probes. The fluorescence of tryptophan almost always dominates in proteins having both types of aromatic residues [4]. In aqueous solution, Tyr and Trp present an emission maximum at 303 nm and 348 nm, respectively [5]. After exciting at 277 nm, the fluorescence emission spectrum of BSA in buffer (pH=7.4) shows a maximum at 347 nm. In this case, Tyr and Trp residues are excited, but the wavelength of maximum emission fluorescence is in concordance with Trp fluorescence. Selective excitation of Trp at 295 nm also shows an emission maximum at 347 nm, but the Raman scatter peak intensity from the solvent was higher than the BSA intensity.

IMA is non-fluorescent under the studied conditions.

3.3. Fluorescence quenching

A fluorescence quenching study of BSA by IMA was performed. For this purpose, solutions of BSA with and without IMA were excited at 277 nm. Fluorescence quenching is a suitable technique to study the possible interaction between IMA and BSA because

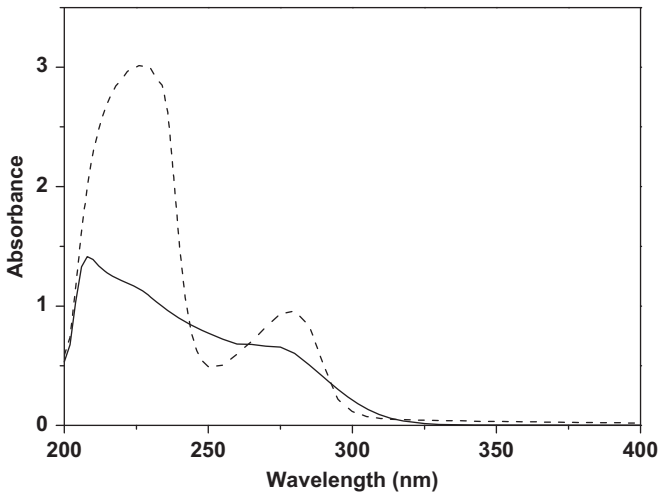

Fig. 2. Absorption spectra of IMA (solid line) and BSA (dotted line). [IMA]=9.44×10^{-5} M; [BSA]=2.56×10^{-5} M.

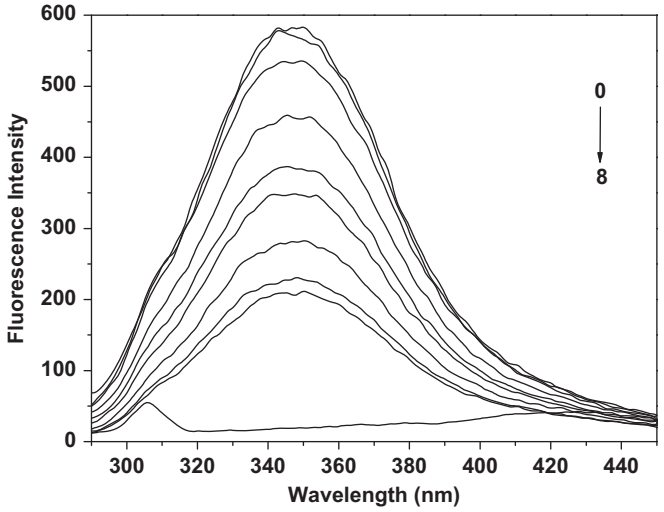

Fig. 3. Fluorescence quenching of BSA by IMA. λ_{exc}=277 nm; [BSA]=2.04×10^{-7} M; [IMA] 0–8=0, 3.72×10^{-6}, 7.44×10^{-6}, 1.86×10^{-5}, 2.98×10^{-5}, 4.09×10^{-5}, 6.33×10^{-5}, 8.19×10^{-5} and 9.31×10^{-5} M; Tris–HCl spectrum is shown.

BSA has two Trp residues (134 and 212) as intrinsic fluorophores. The position of the fluorescence emission maximum (λ_{max}) depends on the properties of the environment of the Trp residues. On the other hand, fluorescence intensity depends on the exposure of the Trp side chains to solvent and its proximity to specific quenchers.

Fig. 3 shows the fluorescence quenching of BSA by IMA. The emission maximum of BSA is not modified in presence of IMA, indicating that the properties around the Trp residues are not changed. A λ_{max}=347 nm is characteristic of Trp fluorescence. At the working pH, IMA has some ionized groups as its pKa values (pKa_1=2.1, pKa_2=3.9) can reveal. For this reason, the accessibility of Trp residues to IMA is limited to superficial Trp because of the presence of charged groups. Trp-212 is in a non-solvent-exposure environment and IMA cannot penetrate into the hydrophobic structure of the BSA to quench Trp-212 fluorescence.

The progressive decrease in fluorescence intensity with increasing concentration of IMA can be explained by three possible mechanisms: (i) inner filter effect; (ii) collisional quenching and (iii) binding-related changes in fluorescence (static, dynamic or a combination of both) [6].

In order to remove the first mechanism, fluorescence intensities were corrected for inner filter effects using the following equation [7,8]:

$$F_{corr} = F_{obs}\ \text{antilog}\ [(A_{ex}+A_{em})/2] \quad (1)$$

where F_{obs} and F_{corr} are the observed and corrected fluorescence intensities, respectively (in a 1.0 cm pathlength cell). A_{ex} and A_{em} are the absorbances at exciting and emission wavelength, respectively (in a 1.0 cm pathlength cell).

Fig. 4 shows the fluorescence intensity of BSA in presence of IMA, with and without correction for inner filter effects. After the removal of inner filter effects, it is evident that the observed reduction in the fluorescence intensity of BSA is related to either collisional quenching or a binding-related process.

3.4. Mechanism of fluorescence quenching

There are two types of quenching mechanisms that characterize the interaction between quenchers and macromolecules: static and dynamic. Static quenching refers to the formation of a ground state non-fluorescence fluorophore–quencher complex. In dynamic quenching, the quencher must diffuse to the fluorophore during the lifetime of the excited state and returns to the ground state, without emission of a photon. The diffusion of the quencher to the fluorophore can lead to collisional quenching or FRET. Collisional quenching requires molecular contact between the fluorophore and the quencher, while FRET needs them to be at a specific distance to occur.

Static and dynamic quenching can be distinguished by their differing dependence on temperature and viscosity. Higher temperatures result in faster diffusion and hence larger amounts of dynamic quenching. On the other hand, higher temperatures will typically result in the dissociation of weakly bound complexes, and hence smaller amounts of static quenching. The measurement of fluorescence lifetimes is the most definitive method to distinguish static and dynamic quenching. Static quenching removes a fraction of the fluorophores from observation. The complexed fluorophores are nonfluorescent, and the only observed fluorescence is from the uncomplexed fluorophores. The uncomplexed fraction is unperturbed, and hence the lifetime is τ_o. Therefore, for static quenching $\tau_o/\tau = 1$. In contrast, for dynamic quenching $F_o/F = \tau_o/\tau$. The decrease in lifetime occurs because quenching is an additional rate process that depopulates the excited state [7].

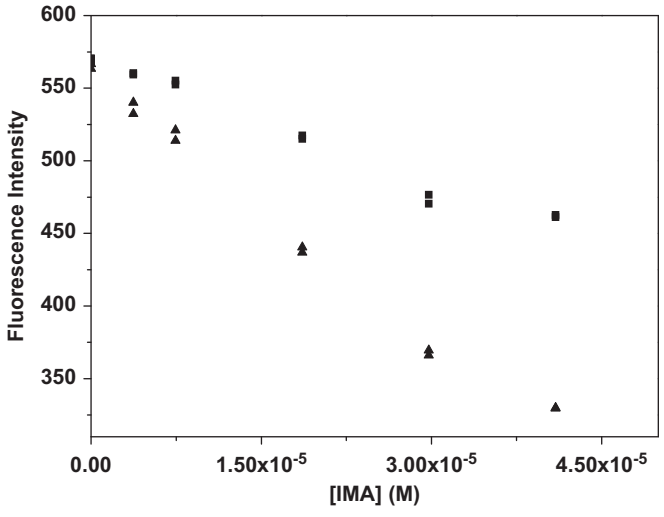

Fig. 4. Fluorescence intensity of BSA in presence of IMA, with (■) and without (▲) correction for inner filter effects.

Dynamic (collisional) quenching can be studied using the Stern–Volmer equation

$$\frac{F_o}{F} = 1 + k_q\tau_o[Q] = 1 + K_D[Q] \quad (2)$$

where F_o and F are the fluorescence intensities in the absence and presence of quencher, respectively; k_q is the bimolecular (or dynamic) quenching constant; τ_o is the lifetime of BSA in the absence of quencher and [Q] is the concentration of quencher. The Stern–Volmer quenching constant is given by $K_D = k_q\tau_o$. If the quenching is known to be dynamic, the Stern–Volmer constant will be represented by K_D. Otherwise, this constant will be described as K_{SV} [7]. The Stern–Volmer equation requires that the added quencher concentration can be approximated as the free ligand concentration (this situation is achieved if the added ligand concentration is much larger than the protein concentration) and the formed complex must be non-fluorescent. Eq. (2) can be used to determine K_{SV} from a linear plot of F_o/F vs [Q].

A linear Stern–Volmer plot is generally indicative of a single class of fluorophores, all equally accessible to quencher. If two fluorophore populations are present, and one class is not accessible to quencher, then the Stern–Volmer plots deviate from linearity toward the *x*-axis. This result is frequently found for the quenching of tryptophan fluorescence in proteins by polar or charged quenchers. These molecules do not readily penetrate the hydrophobic interior of proteins, and only those tryptophan residues on the surface of the protein are quenched [7].

The dynamic quenching rate constant, k_q, will be the product of the quenching efficiency, γ, times the diffusion-limited bimolecular rate constant for collision, k. The value of k can be theoretically calculated by use of the Smoluchowski equation (here we neglect the transient term)

$$k_q = \gamma k \quad (3)$$

$$k = 4\pi D R_o N' \quad (4)$$

where D and R_o are the sum of the diffusion coefficients and molecular radii, respectively, of the quencher and fluorophore, and N' is Avogadro's number divided by 1000. The diffusion coefficient for each species can be predicted by the Stokes–Einstein equation

$$D_i = \frac{k_B T}{6\pi R\eta} \quad (5)$$

where η is the solvent viscosity, k_B is Boltzmann's constant, T is the absolute temperature and R is the radius of the species. Thus, for an efficient collisional quencher, k_q is expected to vary with T/η [9]. In contrast, for a static quenching mechanism (a process that does not involve diffusion), k_q is not expected to vary with $1/\eta$, and hence with F_o/F.

In order to determine the involved quenching mechanism, fluorescence intensities were measured at three temperatures.

Inner filter effects correction was performed. The dependence of the molar absorption coefficient, $\varepsilon(\lambda)$, on temperature was verified first. For this purpose, absorbances of three solutions (BSA, IMA and BSA+IMA) were measured at three temperatures (22.5, 25.8 and 30 °C) and at three wavelengths (277, 295 and 347 nm). The third solution (BSA+IMA) confirmed absorbance additivity. The obtained results indicate that the molar absorption coefficient is not a function of the temperature in the studied range. Based on this result, absorbances were measured at room temperature in order to correct the observed fluorescence intensities.

For solutions in which the absorbance does not exceed a value of 0.3, inner filter effects can be corrected using Eq. (1) [10]. Fig. 5 shows the Stern–Volmer plots at three temperatures, corrected for inner filter effects, in the linear range. Experimentally, concentrations up to 1.73×10^{-4} M (data not shown) were reached.

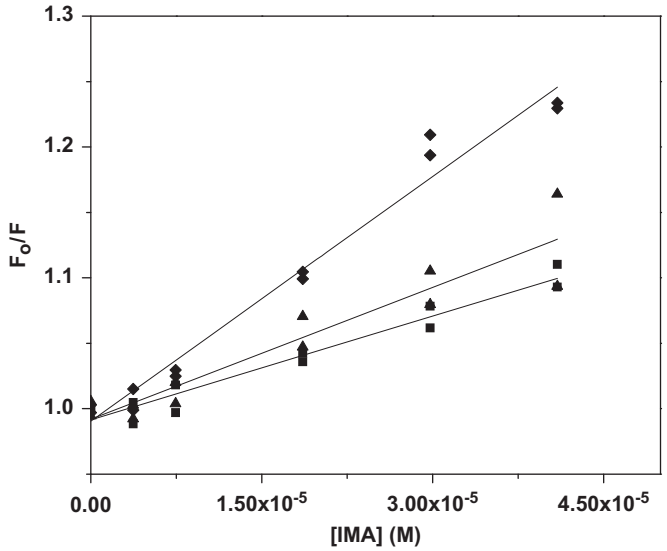

Fig. 5. Stern–Volmer plots at 293 K (♦), 300 K (▲) and 306 K (■).

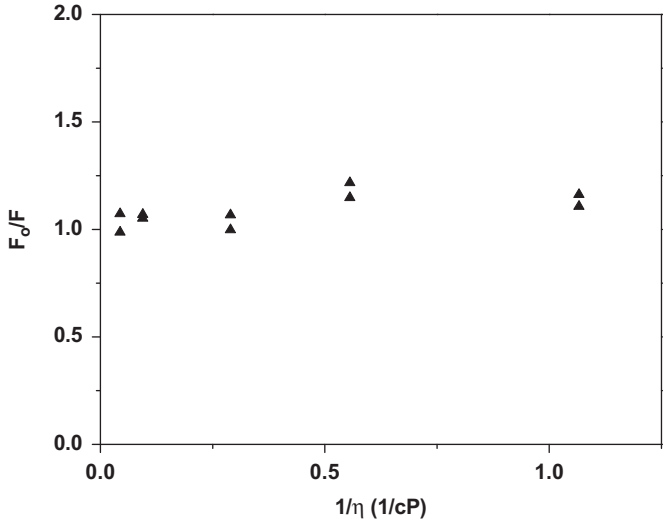

Fig. 6. F_o/F as a function of viscosity; [BSA]$=2.06\times10^{-7}$ M; [IMA]$=2.98\times10^{-5}$ M; [sucrose]$=0$, 20, 40, 60 and 70%. Dots (▲ or ■) at the same viscosity represent duplicate values.

Table 1
Stern–Volmer constants at three temperatures.

T	293 K	300 K	306 K
K_{SV} (M^{-1})	6233	3358	2639

A downward curvature was observed for concentrations of IMA where the absorbance values were greater than 0.3. Because of the impossibility of using Eq. (1) to correct for inner filter effect, we cannot give a certain conclusion about the cause of the downward curvature observed. Table 1 summarizes the obtained values for the Stern–Volmer constant. As can be appreciated, at higher temperatures the value of K_{SV} decreases indicating a static quenching mechanism.

The dependence of fluorescence quenching on viscosity was also evaluated in order to confirm the involved quenching mechanism. For this purpose, viscosity of BSA and IMA solutions was varied by adding increasing concentrations of sucrose (0–70%). Viscosity was measured using an Ostwald viscometer. Fig. 6 shows that there is a negligible variation in the ratio F_o/F with viscosity, and hence with k_q, indicating that the mechanism of fluorescence quenching is static. Lifetime measurements could not be performed because of the lack of the appropriate instrument.

3.5. Binding constant and binding sites

For the static quenching process, under the assumption that there are same and independent binding sites n in the protein, that is, at each binding site there is the same capacity for the BSA binding with the quencher, the reaction is

$$P+nD\rightarrow D_nP \tag{6}$$

where P is the protein, D is the quencher and D_nP is the new complex molecule whose binding constant is K_A. The binding constant and the number of binding sites (n) can be calculated using the following equation:

$$\log\frac{(F_o-F)}{F}=n\log K_A-n\log\left\{\frac{1}{[D_t][(F_o-F)[P_t]]/F_o}\right\} \tag{7}$$

where F_o and F are the fluorescence intensities in the absence and presence of quencher, $[P_t]$ is the total concentration of protein and $[D_t]$ is the total concentration of quencher. By the plot of

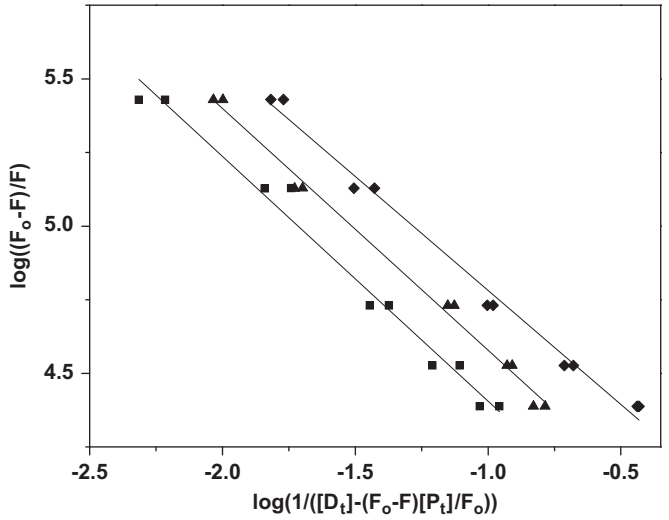

Fig. 7. Plots of $\log(F_o-F)/F$ vs $\log\{1/\{[D_t]-(F_o-F)[P_t]/F_o\}\}$ at 293 K (♦), 300 K (▲) and 306 K (■).

Table 2
Values of K_A and n for the interaction BSA–IMA at three temperatures.

T	293 K	300 K	306 K
n	0.77	0.82	0.83
K_A (M^{-1})	1.51×10^5	3.77×10^4	1.98×10^4

$\log(F_o-F)/F$ vs $\log\{1/\{[D_t]-(F_o-F)[P_t]/F_o\}\}$, the number of binding sites n and binding constant K_A can be obtained [11].

The assumption of n equal and independent binding sites in the protein is satisfied in the studied case: Trp-212 is not quenched by the ionized herbicide at pH=7.4 resulting in the existence of one binding site (Trp-134).

Fig. 7 shows the plots at three temperatures and Table 2 summarizes the obtained results.

3.6. Binding modes

The acting forces between a small molecule and a biomolecule are composed of weak interactions such as hydrogen bond

Table 3
Values of K_A and n for the interaction BSA–IMA at three temperatures.

	$\Delta G^{293\ K}$ (kJ mol^{-1})	$\Delta G^{300\ K}$ (kJ mol^{-1})	$\Delta G^{306\ K}$ (kJ mol^{-1})	ΔH (kJ mol^{-1})	ΔS (J mol^{-1} K^{-1})
BSA–Imazethapyr	−28.85	−26.73	−24.92	−117.24	−301.69

formation, van der Waals forces, electrostatic forces, and hydrophobic interaction [12]. The thermodynamic parameters, enthalpy (ΔH) and entropy changes (ΔS), for the binding reaction are the main evidence to confirm binding modes. From the thermodynamic standpoint, $\Delta H > 0$ and $\Delta S > 0$ imply a hydrophobic interaction; $\Delta H < 0$ and $\Delta S < 0$ reflect the van der Waals forces or hydrogen bond formation; and $\Delta H \approx 0$ and $\Delta S > 0$ suggest an electrostatic force [13].

For this purpose, the temperature dependence on the binding constant can be studied at three different temperatures in the range of no protein structural degradation. The thermodynamic parameters can be calculated on the basis of the van't Hoff equation

$$\ln K = -\frac{\Delta H}{RT} + \frac{\Delta S}{R} \tag{8}$$

where K is the binding constant at the corresponding temperature, T, and R is the gas constant. The enthalpy change (ΔH) and entropy change (ΔS) are calculated from the plot of ln K vs $1/T$. The free energy change (ΔG) can be estimated from the following relationship:

$$\Delta G = -RT \ln K = \Delta H - T\Delta S \tag{9}$$

A negative sign for ΔG reveals that the binding process is spontaneous.

Table 3 shows the obtained results. The negative values of ΔG and ΔH reflect a spontaneous and exothermic binding process, with negative values of ΔS. The negative values of ΔH and ΔS imply that hydrogen bonds and van der Waals forces play an important role in the binding process.

3.7. Quenching by KI

The quenching of protein fluorescence by iodide ion has been extensively used to probe the accessibility of tryptophan residues in proteins and the change in accessibility induced by ligand binding [14]. BSA has two Trp residues: Trp-212 and Trp-134. Trp-134 is more solvent-exposed than Trp-212. As stated earlier, BSA exhibits maximum fluorescence emission intensity at 347 nm, characteristic of proteins that have fully surface exposed tryptophans. KI is a highly hydrated and charged quencher that cannot penetrate the hydrophobic structure of the protein, resulting in the specific quenching of the Trp residues exposed to the solvent.

KI quenching was performed by the addition of small aliquots of 2 M KI. The iodide solution contained sodium thiosulphate (5×10^{-4} M) to suppress tri-iodide formation. The fluorescence emission intensities were corrected for inner filter effects. The emission maximum of BSA is not modified in presence of KI, indicating that the properties around the Trp residues are not changed. The Stern–Volmer plots are shown in Fig. 8. The points could not pass through a single line, indicating heterogeneity of Trp residues [14]. The k_q value for BSA with IMA was slightly lower than k_q for BSA alone. Based on this result, it is possible that binding of BSA with IMA causes a structural change that buried the exposed Trp-134 residues of BSA or IMA binds to BSA in the site where Trp-134 is located, causing it to be sandwiched and so becomes less exposed to the solvent [15]. The emission maximum of BSA ($\lambda = 347$ nm) is not affected in the presence of increasing concentrations of KI, excluding the possibility of structural changes in BSA. The reason of a lower k_q value for BSA with IMA than for BSA alone is the formation of a complex between IMA and BSA that causes the Trp-134 residues to become less exposed to the solvent.

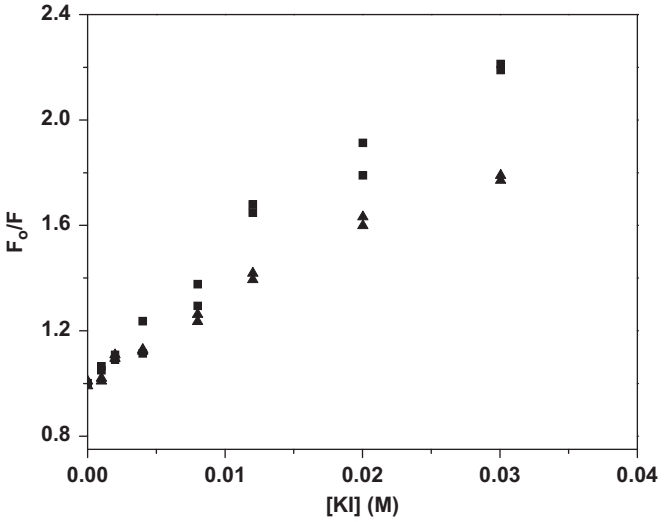

Fig. 8. Stern–Volmer plots in presence (▲) and absence (■) of IMA.

4. Conclusions

The interaction between IMA and BSA was investigated by means of steady state fluorescence spectroscopy. Based on the obtained results, the fluorescence quenching mechanism of BSA by IMA is static. The binding process is spontaneous and exothermic, and hydrogen bonds and van der Waals forces are the dominant forces in the interaction between BSA and IMA. Accessibility of tryptophan residues in BSA revealed that IMA forms a complex in the site where Trp-134 is located.

Acknowledgments

The authors thank Facultad de Ciencias Exactas, Universidad Nacional de La Plata, Argentina, for partial financial support. M.E.P. acknowledges Comisión de Investigaciones Científicas (CIC) de la Provincia de Buenos Aires, Argentina.

References

[1] D.C. Carter, J.X. Ho, Adv. Protein Chem. 45 (1994) 153.
[2] X.M. He, D.C. Carter, Nature 358 (1992) 209.
[3] S. Hamdani, D. Joly, R. Carpentier, H.A. Tajmir-Riahi, J. Mol. Struct. 936 (2009) 80.
[4] M.R. Eftink, in: J.R. Lakowicz (Ed.), Topics in Fluorescence Spectroscopy, 6, Kluwer Academic Publishers, 2002.
[5] S.V. Konev, Fluorescence and Phosphorescence of Proteins and Nucleic Acids, Plenum Press, New York, 1967.
[6] M. van de Weert, L. Stella, J. Mol. Struct. 998 (2011) 144.
[7] J.R. Lakowicz, Principles of Fluorescence Spectroscopy, third ed., Springer Publisher, New York, 2006.

[8] C.A. Parker, Photoluminescence of Solutions, Elsevier Publishing Company, Amsterdam, 1968.
[9] M.R. Eftink, in: J.R. Lakowicz (Ed.), Topics in Fluorescence Spectroscopy, 2, Kluwer Academic Publishers, 2002.
[10] E.P. Kirby, Excited States of Proteins and Nucleic Acids, in: R.F. Steiner, L. Weinryb (Eds.), Plenum Press, 1971.
[11] S. Bi, L. Ding, Y. Tian, D. Song, X. Zhou, X. Liu, H. Zhang, J. Mol. Struct. 703 (2004) 37.
[12] D.A. Leckband, Annu. Rev. Biophys. Biomol. Struct. 29 (2000) 1.
[13] P.D. Ross, S. Subramanian, Biochemistry 20 (1981) 3096.
[14] M.K. Das, M.I. Khan, A. Surolia, Biochem. J. 195 (1981) 341.
[15] N.S. Quiming, R.B. Vergel, M.G. Nicolas, J.A. Villanueva, J. Health Sci. 51 (2005) 8.